



Semi-Classical Infrared Emission Processes
in the $(\phi^4)_4$ Theory

SHAU-JIN CHANG*

Fermi National Accelerator Laboratory, Batavia, Illinois 60510 †
and
Physics Department, University of Illinois, Urbana, Illinois 61801

YORK-PENG YAO ‡

Fermi National Accelerator Laboratory, Batavia, Illinois 60510 †
and
Randall Laboratory of Physics, University of Michigan,
Ann Arbor, Michigan 48109

INGA KARLINER*

Physics Department, University of Illinois. Urbana, Illinois 61801

*Supported in part by the National Science Foundation under Grant No. NSF Phy 75-21590.

† Operated by Universities Research Association, Inc. under contract with the Energy Research and Development Administration.

‡ Work supported in part by the U. S. E. R. D. A.



ABSTRACT

We consider the decay of a time-like gluon into soft gluons in a $(\phi^4)_4$ theory. We make a semiclassical approximation by keeping only the diagonal tree diagrams. We are able to determine the dominant features of the soft gluon emissions by examining the decay amplitude in the position space. We have obtained the asymptotic decay rate, the average multiplicity and moments of the multiplicity for the final gluons. In particular, we find that in the strong coupling limit all the energy of the original time-like gluon is turned into emission of soft gluons at rest.

I. INTRODUCTION

In this article, we report some results from our continual study of the infrared behaviors of massless theories with self-coupling. Although our ultimate aim is to understand the infrared structure of non-abelian gauge theories at this stage of development, our emphasis is still more on methodology.

Let us recall that in Ref. 1, we have observed that, because of self-interaction, a massless gluon can successively split into many gluons. If the coupling constant can be made arbitrarily large, then none but soft gluons can be excited from a physical system, where by soft we mean their energies to be lower than any arbitrary resolution. We envisage this as a viable mechanism to prohibit hard gluons from being produced. The soft gluons may either materialize into hadrons or act coherently as parts of the self-fields of the parents from which they emanate.

We shall apply this same consideration to a scalar gluon ϕ in four dimensional space, which interacts via $\frac{\lambda}{4!} \phi^4$. We should hasten to qualify our limited scope in this investigation. It is known that $(\phi^4)_4$ is an infrared stable theory² and hence it will not be meaningful to take the strong coupling limit to study its infrared content in the context of the full theory. We certainly concur with this sentiment. However, we shall limit ourselves to a study at the tree level only.

This, as explained earlier, is but an example to develop new tools. If the reader prefers, he may choose to regard ϕ^4 to be a simplified form of the quadrilinear coupling which appears in non-abelian gauge theories. If, with this understanding, the strong coupling limit is approached, the aforementioned mechanism again is seen at work.

We may also recall that the analysis in Ref. 1 is somewhat tedious. We have succeeded in developing a new method, which shortens the whole procedure drastically. The crucial observation is to note that it helps to work in the Euclidian coordinate space. The absorptive part of the true point function $\tilde{F}(x)$, which is the Fourier transform of what we called the inclusive dissociation probability $F(p^2)$, is real in this regime. It turns out that the singularity (or pole) furthestmost away from the origin along the real positive axis of $x^2 = -x_\mu x^\mu$ determines the leading infrared behavior in the time-like region $p^2 > 0$ of $F(p^2)$. Thus, by working directly with an integral equation in x^2 , we can extract the leading infrared behavior in p^2 with great ease. This has the extra merit of rendering the analysis transparent.

The plan of this paper is as follows. In the next section, we briefly discuss the diagonal free approximation and write down an integral equation so obtained. Sec. III is the novel part of this work, where, after introducing spectral representation for the two point function

$\langle \phi^{(+)}(x) \phi^{(-)}(0) \rangle$, we observe that for space-like separation it is a Fourier-Bessel transform. The inverse transform has the property

that $F(p^2)$ for $p/\mu \gg 1$ is governed by the furthestmost singularity of $\tilde{F}(x)$. $\tilde{F}(x)$ is then analytically continued into the Euclidian region of x^2 and a radial differential equation is generated, which can be easily converted into an integral equation.

In Sec. IV, we discuss the nature of our intention and write down analytic expressions for the position of the governing pole of $\tilde{F}(x)$, β , in the large and small coupling limits. The distribution properties of soft emission processes are briefly touched on.

Lastly, a summary of the scope of our work in this area is presented and further obstacles to be overcome in order to solve the corresponding problem in non-abelian gauge theories are exposed.

An appendix is prepared, where the mathematical details to determine β analytically are given.

II. DIAGONAL TREE DIAGRAMS

In this paper, we study the total decay rate for a time-like scalar gluon of momentum $p(p^2 > 0)$ under the self interaction $\frac{\lambda}{4!} \phi^4$. We restrict ourselves to the diagonal tree diagrams such as in Fig. 1. Just as in the $(\phi^3)_6$ theory discussed in paper I, the diagonal tree diagrams in the $(\phi^4)_4$ theory also bound the full tree diagrams from below. In the small coupling limit, the diagonal tree diagrams give the leading infrared contribution of the full tree diagrams in every order of perturbation theory.

The diagonal tree diagram $F(p^2)$ obeys an integral equation

$$F(p^2) = 2\pi \delta(p^2 - \mu^2) + \frac{\lambda^2}{6} \frac{1}{(p^2 - \mu^2)^2} \int \frac{d^4 q_1}{(2\pi)^4} \frac{d^4 q_2}{(2\pi)^4} \frac{d^4 q_3}{(2\pi)^4} \quad (2.1)$$

$$\times (2\pi)^4 \delta^{(4)}(q_1 + q_2 + q_3 - p) F(q_1^2) F(q_2^2) F(q_3^2)$$

with

$$F(p^2) = 0 \quad \text{for} \quad p^2 < \mu^2, \text{ or } p^0 < 0. \quad (2.2)$$

This integral equation is shown graphically in Fig. 2. Eq. (2.2) is an analog of Eq. (A-11) in Appendix A of paper I, and can be derived by the same method. We refer the readers to paper I for detailed discussions. The mass parameter μ^2 is introduced as an infrared cutoff and will be made arbitrarily small. Since only three or more gluon final states can contribute to the second term of (2.1), p^2 appearing in the second term must always be larger than $9\mu^2$. To study the infrared behavior of $F(p^2)$ it is a good approximation to ignore μ^2 in the propagators in the second term. We then obtain the approximate integral equation

$$F(p^2) = 2\pi \delta(p^2 - \mu^2) + \frac{\lambda^2}{6p^4} \int \frac{d^4 q_1}{(2\pi)^4} \frac{d^4 q_2}{(2\pi)^4} \frac{d^4 q_3}{(2\pi)^4}$$

$$\times (2\pi)^4 \delta^{(4)}(q_1 + q_2 + q_3 - p) F(q_1^2) F(q_2^2) F(q_3^2). \quad (2.3)$$

One can show that Eq. (2.3) gives rise to the correct small and large

λ solution.

III. COORDINATE SPACE FORMULATION AND THE BESSEL TRANSFORM.

In paper I we showed that the large p/μ (or, equivalently the small μ/p) behavior of $F(p^2)$ is of the form

$$F(p^2) = A p^\alpha e^{\beta p} \quad (3.1)$$

where the exponent β is a function of the coupling constant λ . We have determined the upper and lower bounds of β using the method of Laplace transform. We refer the readers to paper I for details. In this section, we will develop a new method which relates β to the position of a pole in the Bessel transform of $\tilde{F}(x)$. The method of Bessel transform enables us to study β most directly.

(a) x-space Amplitude

We define the x-space amplitude as

$$\tilde{F}(x) \equiv \int \frac{d^4 p}{(2\pi)^4} e^{ip \cdot x} F(p^2) \quad (3.2)$$

For a time-like x_μ , \tilde{F} is a function of both x^2 and $\text{sign}(x^0)$. For a space-like x , \tilde{F} is a function of x^2 only. It turns out that, to study $F(p^2)$ for time-like p^2 , we only need to know \tilde{F} for space-like x^2 . In x-space, we can write (2.1) as

$$\tilde{F}(x) = \tilde{F}_0(x) + \frac{\lambda^2}{6} (\partial^2 + \mu^2)^{-2} \tilde{F}(x)^3 \quad (3.3)$$

where $(\partial^2 + \mu^2)^{-1}$ is a short-hand notation for x-space Green's function,

and

$$\begin{aligned}\tilde{F}_0(x) &\equiv \int \frac{d^4 p}{(2\pi)^4} e^{ip \cdot x} 2\pi \delta(p^2 - \mu^2) \\ &= \frac{\mu K_1(\mu x)}{4\pi^2 x} \quad \text{for spacelike } x \\ &\quad \text{with } x_\mu x^\mu = -x^2.\end{aligned}\quad (3.4)$$

Note that $\tilde{F}_0(x)$ is a solution of the free field equation

$$(\partial^2 + \mu^2) \tilde{F}_0(x) = 0. \quad (3.5)$$

We can write (3.3) as

$$(\partial^2 + \mu^2)^2 \tilde{F}(x) = \frac{\lambda^2}{6} \tilde{F}(x)^3 \quad (3.6)$$

with the boundary condition

$$\lim_{x^2 \rightarrow \infty} \tilde{F}(x) = \tilde{F}_0(x). \quad (3.7)$$

Under the same approximation which leads to (2.3), we have

$$\partial^4 \tilde{F}(x) = \mu^4 \tilde{F}_0(x) + \frac{\lambda^2}{6} \tilde{F}(x)^3 \quad (3.8)$$

with the same boundary condition (3.7). In the remaining part of this paper, we shall study the solutions to Eqs. (2.3) or equivalently, (3.8).

(b) Bessel Transform

Knowing $F(p^2)$ for all time-like p , we can determine $\tilde{F}(x)$ for a space-like x by a Bessel transform. Conversely, knowing $\tilde{F}(x)$ for a

for space-like x 's, we can determine $F(p^2)$ for a time-like p by an inverse Bessel transform.

From Eq. (3.2), we have

$$\begin{aligned}\tilde{F}(x) &= \int_0^\infty \frac{dm^2}{2\pi} F(m^2) \int \frac{d^4p}{(2\pi)^4} e^{ip \cdot x} 2\pi \delta(p^2 - m^2) \\ &= \int_0^\infty \frac{dm^2}{2\pi} F(m^2) \frac{m K_1(mx)}{4\pi^2 x}\end{aligned}\quad (3.9)$$

with

$$x_\mu x^\mu \equiv -x^2 < 0.$$

We can cast (3.9) into the standard Bessel transform³

$$4\pi^3 x^{3/2} \tilde{F}(x) = \int_0^\infty dm (mx)^{\frac{1}{2}} K_1(mx) m^{3/2} F(m^2). \quad (3.10)$$

The inverse transform of (3.10) is well-known, and is given by

$$m^{3/2} F(m^2) = \frac{1}{i\pi} \int_{c-i\infty}^{c+i\infty} dx (mx)^{\frac{1}{2}} I_1(mx) 4\pi^3 x^{3/2} \tilde{F}(x) \quad (3.11)$$

where the contour c is on the right of all the singularities of $x^{3/2} \tilde{F}(x)$.

It is easy to see that if $F(p^2) \sim e^{\beta p}$ at large p , $\tilde{F}(x)$ develops a singularity at $x = \beta$. Conversely, the large p behavior of $F(p^2)$ is dominated by the furthest singularity of $\tilde{F}(x)$, i. e., if $\tilde{F}(x)$ has the furthest singularity at $x = \beta$ then, $F \sim e^{\beta p}$ at large p . For this reason, we only need to study the furthest singularity of $\tilde{F}(x)$ to determine the exponent β .

(c) Radial Equation

For space-like x , we can analytically continue (3.8) into Euclidean region. Then, $\tilde{F}(x)$ is spherically symmetric, and obeys the equation

$$\left(\frac{d^2}{dr^2} + \frac{3}{r} \frac{d}{dr}\right)^2 \tilde{F}(r) = \mu^4 \tilde{F}_0(r) + \frac{\lambda^2}{6} \tilde{F}(r)^3 \quad (3.12)$$

where

$$\tilde{F}_0(r) = \frac{\mu K_1(\mu r)}{4\pi^2 r} \quad (3.13)$$

obeys the free equation

$$\left(\frac{d^2}{dr^2} + \frac{3}{r} \frac{d}{dr} + \mu^2\right) \tilde{F}_0(r) = 0. \quad (3.14)$$

Next we wish to rewrite (3.12) as an integral equation. We introduce a Green's function G which obeys

$$-\left(\frac{d^2}{dr^2} + \frac{3}{r} \frac{d}{dr}\right) G(r, r') = \delta(r - r'), \quad (3.15)$$

$$G(r, r') = 0, \quad r > r'. \quad (3.16)$$

The Green's function satisfying (3.15) and (3.16) is

$$G(r, r') = \frac{1}{2} \left(r' - \frac{r'^3}{r^2}\right) \theta(r' - r). \quad (3.17)$$

Using (3.15) - (3.17), we can convert (3.12) into an integral equation

$$\tilde{F}(r) = \tilde{F}_0(r) + \frac{\lambda^2}{6} \int_0^\infty dr' G^2(r, r') \tilde{F}(r')^3 \quad (3.18)$$

where

$$G^2(r, r') \equiv \int_0^\infty dr'' G(r, r'') G(r'', r')$$

$$= \frac{1}{16} \left(\frac{r'^5}{r^2} - r' r^2 - 4 r'^3 \ln r'/r \right) \theta(r' - r). \quad (3.19)$$

Note that the boundary condition (3.7) is satisfied automatically in this integral representation. We shall use (3.18) to determine β . Using the method of Appendix B in paper I, we can show that $\tilde{F}(r)$ develops a singularity at non-vanishing β ($\beta \neq 0$) no matter how small the λ is.

IV. NATURE OF THE SOLUTION AND THE DISTRIBUTION PROPERTIES

(a) Structure of the Solution

We can determine the large p/μ (or small μ) behavior of the solution once the exponent β is given. We can achieve this result by using the asymptotic form

$$F(p^2) = A p^n e^{\beta p^2} \quad (4.1)$$

and substitute it into Eq. (2.3). After integrating out the angular variables on the right-hand side of (2.3) we compare the p^n and A terms on both sides of Eq. (2.3), and obtain

$$n = -1/2 \quad (4.2)$$

and

$$A = \sqrt{6! (2\pi)^5 \beta^3} / \lambda. \quad (4.3)$$

Thus, we can express F as

$$F(p^2) = \frac{\sqrt{6! (2\pi)^5}}{\lambda} \frac{1}{p^2} (\beta p)^{3/2} e^{\beta p}. \quad (4.4)$$

This result can also be obtained by examining the property of $\tilde{F}(r)$ near the singularity $r = \beta$.

As we have demonstrated in paper I, we can obtain all distribution properties via $F(p)$ once β is known.

(b) Determination of β

We can determine the small and large λ behaviors of β explicitly, the derivation of which is left to an Appendix. The results can be summarized as: (1) for small λ we have

$$\beta \mu = \text{const.} \exp \left[- \frac{48 (2\pi)^4}{\lambda^2} \right], \quad \lambda \ll 1. \quad (4.5)$$

It is more convenient to introduce a new coupling constant g via

$$g^2 = \frac{\lambda^2}{48 (2\pi)^4}. \quad (4.6)$$

Then we have

$$\chi_0 \equiv \beta \mu = \text{const.} e^{-1/g^2}, \quad g \ll 1. \quad (4.7)$$

Note that β develops an essential singularity at $g=0$, and it can not be obtained by simple perturbation expansion. (2) For large λ (or g), we have

$$X_0 \equiv \beta \mu = b(\lambda) + \text{const.} \quad \lambda \gg 1 \quad (4.8)$$

with b obeying

$$b + \frac{3}{2} \ln b = \ln \lambda. \quad (4.9)$$

We can also express the result in terms of g as well.

$$X_0 \equiv \beta \mu = b'(g) + \text{const.} \quad g \gg 1 \quad (4.10)$$

with

$$b' + \frac{3}{2} \ln b' = \ln g. \quad (4.11)$$

(3) For intermediate values of λ (or g), we have obtained β by solving the integral equation (3.18). The results are expressed numerically in Figs. (3) and (4). The numerical results agree with the exact strong and weak coupling behaviors in their corresponding limits.

(c) Multiplicity Distribution

As we have shown in paper I, we can compute the average multiplicity and various moments once β is known. An important difference between the ϕ^3 and ϕ^4 tree diagrams is that in a ϕ^3 theory every tree vertex leads to an additional final particle, while in a ϕ^4 theory every tree vertex leads to two additional particles. This difference leads to the following modified formulae:

$$\langle n \rangle = 2g^2 \frac{\partial}{\partial g^2} \ln F = g \frac{\partial \beta}{\partial g} \cdot p + \text{const.}, \quad (4.12)$$

$$\begin{aligned} \langle n^2 \rangle - \langle n \rangle^2 &= 4 \left(g^2 \frac{\partial}{\partial g^2} \right)^2 \ln F \\ &= \left(g \frac{\partial}{\partial g} \right)^2 \beta(g) \cdot p + \text{const.}, \dots \end{aligned} \quad (4.13)$$

The constant terms are negligible in the large p/μ limit.

At small g (or λ), we have

$$\beta = \frac{\text{const.}}{\mu} \cdot \exp\left(-\frac{1}{g^2}\right),$$

and consequently,

$$\langle n \rangle = \frac{2}{g^2} \exp\left(-\frac{1}{g^2}\right) \frac{p}{\mu}, \quad (4.14)$$

$$\langle n^2 \rangle - \langle n \rangle^2 = 4 \left(\frac{1}{g^4} - \frac{1}{g^2} \right) \exp\left(-\frac{1}{g^2}\right) \frac{p}{\mu}. \quad (4.15)$$

At large g , we have

$$\beta = \frac{1}{\mu} \left[\ln g - \frac{3}{2} \ln(\ln g) + \dots \right], \quad (4.16)$$

$$\langle n \rangle = \left(1 - \frac{3}{2} \frac{1}{\ln g} \right) \frac{p}{\mu}, \quad (4.17)$$

and

$$\langle n^2 \rangle - \langle n \rangle^2 = \frac{3}{2 (\ln g)^2} \cdot \frac{p}{\mu}. \quad (4.18)$$

As in the $(\phi^3)_6$ case, the multiplicity reaches the maximally allowed

value p/μ at the large g limit. In Figs. (5) and (6) we have plotted $\langle n \rangle$ and $\langle n^2 \rangle - \langle n \rangle^2$ (normalized to p/μ) for intermediate values of g . Other higher multiplicity moments can be computed in a similar way.

V. DISCUSSION

In this paper, we develop a simple method to study the diagonal tree diagrams. This method is also applicable to other theories. This is to be contrasted with paper I, where we used the Laplace transform method to study the $(\phi^3)_6$ tree amplitudes. In order to apply the Laplace transform method, we had to approximate the phase space integral by an upper and a lower bound. We determined the behavior of the amplitude for both the upper and lower bounds, and thereby obtained the qualitative features of the solutions. In the present paper, we are able to study the asymptotic behavior directly by the use of a Bessel transform. We can, of course, apply the Bessel transform method to $(\phi^3)_6$ and obtain the diagonal tree amplitudes explicitly.

As far as the diagonal tree diagrams are concerned, $(\phi^3)_6$ and $(\phi^4)_4$ theories are very similar. They both have the asymptotic form,

$$F(p^2) = A p^n e^{\beta p}.$$

They also have similar weak and large coupling behaviors. However, as relativistic quantum field theories, $(\phi^3)_6$ and $(\phi^4)_4$ are quite different.

The $(\phi^4)_4$ theory is infrared free.² We expect that the true infrared behaviors of $(\phi^4)_4$ theory is much softer than that given by the tree amplitude because the running coupling constant vanishes at the infrared limit. The large multiplicity ($\langle n \rangle \propto p/\mu$) predicted by the $(\phi^4)_4$ tree diagram is most likely an overestimate. On the other hand, $(\phi^3)_6$ is an asymptotically-free theory⁴, and its running coupling constant becomes large at the infrared limit. We might indeed expect to see a large number of soft gluons ($\langle n \rangle \propto p/\mu$) being emitted for any coupling constant.

The tree diagrams in a non-abelian gauge theory have many features similar to those of the ϕ^3 and ϕ^4 theories: First, both the gauge gluons and the scalar gluons ϕ are self-coupled via three and/or four point vertices. Second, both the non-abelian gauge theory and the $(\phi^3)_6$ theory are renormalizable and asymptotically-free.⁵ However, there are also important differences. In particular, the tree diagrams in a non-abelian gauge theory are not positive-definite, and possible cancellations among off-diagonal terms are crucial to the asymptotic behavior. In a non-abelian gauge theory, the diagonal tree diagrams are neither a lower bound to the tree diagrams, nor gauge invariant; only the full tree diagrams are gauge invariant. Thus, it is essential to study the full tree diagrams in a non-abelian gauge theory. At the moment, we are only able to sum the full tree diagrams of a non-abelian gauge theory in the leading \ln approximation.⁶ However, the leading \ln result does not appear to be relevant at the large p/μ (or small μ) limit. It is therefore

almost imperative to study the true asymptotic behavior of the full tree diagrams in both the non-abelian gauge theory and the self-coupled scalar gluon theories.

APPENDIX

Small and Large Coupling Behavior of β

To study the small and large λ (or g) behavior of β , we start with the differential equation (3.12)

$$\left(\frac{d^2}{dr^2} + \frac{3}{r} \frac{d}{dr}\right)^2 \tilde{F}(r) = \mu^4 \tilde{F}_0(r) + \frac{\lambda^2}{6} \tilde{F}(r)^3 \quad (\text{A.1})$$

with

$$\tilde{F}_0(r) = \frac{\mu K_1(\mu r)}{4\pi^2 r}, \quad (\text{A.2})$$

and determine the position of the singularity of \tilde{F} at small and large λ .

(a) Small g Behavior

For sufficiently large r , the $\mu^4 \tilde{F}_0(r)$ term on the right-hand side of (A.1) dominates, and we have the relation $\tilde{F}(r) = \tilde{F}_0(r)$. The $\tilde{F}(r)^3$ term becomes comparable to $\mu^4 \tilde{F}_0(r)$ at r_1 given by

$$\mu^4 = \frac{\lambda^2}{6} \tilde{F}_0(r_1)^2$$

or equivalently, at

$$\frac{\lambda}{\sqrt{6}} \frac{K_1(\mu r_1)}{4\pi^2 \mu r_1} = 1. \quad (\text{A.3})$$

For small λ , the transition point r_1 (see (A.3)) takes place at

$$\mu r_1 = \frac{\sqrt{\lambda}}{6^{1/4} \cdot 2\pi} \ll 1. \quad (\text{A.4})$$

For $r \ll r_1$, we can ignore the $\mu^4 \tilde{F}_0(r)$ term and obtain

$$\left(\frac{d^2}{dr^2} + \frac{3}{r} \frac{d}{dr} \right)^2 \tilde{F}(r) = \frac{\lambda^2}{6} \tilde{F}(r)^3. \quad (\text{A. 5})$$

Introducing the variables

$$Z = r^2 \tilde{F}(r), \quad y = \ln(\mu r) \quad (\text{A. 6})$$

we have

$$\left(-16 \frac{d}{dy} + 20 \frac{d^2}{dy^2} - 8 \frac{d^3}{dy^3} + \frac{d^4}{dy^4} \right) Z = \frac{\lambda^2}{6} Z^3. \quad (\text{A. 7})$$

We are looking for the solution to (A. 7) with the boundary condition that

near $y = \ln(\mu r_1)$,

$$Z \approx \frac{\mu r K_1(\mu r)}{4\pi^2} \approx \frac{1}{4\pi^2}, \quad (\text{A. 8})$$

$$\frac{dZ}{dy} = O(\lambda^2 Z^3) \ll 1, \quad (\text{A. 9})$$

and

$$\frac{d^2 Z}{dy^2} = O(\lambda^2 Z^2) \frac{dZ}{dy} \ll \left| \frac{dZ}{dy} \right|. \quad (\text{A. 10})$$

Note that for $y \sim \ln(\mu r_1)$ the higher y derivatives in (A. 7) are much smaller than the first derivative. As y decrease, Z starts to increase, and eventually the higher y derivative terms will dominate. However, for sufficiently small λ , Z will be very large ($\sim O(1/\lambda)$) before $\frac{d^2 Z}{dy^2}$ and other higher derivative terms become important. Thus, we are able

to determine the approximate position of the singularity of Z by examining only the linear differential equation

$$-16 \frac{dZ}{dy} = \frac{\lambda^2}{6} Z^3. \quad (\text{A. 11})$$

We can solve (A. 11) readily, obtaining

$$\frac{1}{Z^2} = C + \frac{\lambda^2}{48} y. \quad (\text{A. 12})$$

From the boundary condition (A. 8), we have at small λ

$$C = \frac{1}{(4\pi)^2} \quad (\text{A. 13})$$

and consequently

$$Z = - \frac{1}{\left[\frac{1}{(4\pi)^2} + \frac{\lambda^2}{48} y \right]^{1/2}}. \quad (\text{A. 14})$$

Thus, the position of the singularity of Z is at

$$y_0 = - \frac{48(4\pi)^2}{\lambda^2} = - \frac{1}{g^2} \quad (\text{A. 15})$$

or

$$\beta\mu = e^{y_0} = e^{-1/g^2}. \quad (\text{A. 16})$$

We wish to make two remarks: (1) As we take the higher y derivatives in (A. 7) into account, the functional form of (A. 14) near the singularity changes. However, the position of the singularity is still given

approximately by (A.16). (2) If we take higher order g 's (or λ 's) into account, β is modified to

$$\beta\mu = \text{const.} \exp(-1/g^2). \quad (\text{A.17})$$

Equation (A.17) is the small coupling behavior of β .

(b) Large g Behavior

To obtain the large g (or λ) behavior, we go back to the original equation (A.1). After making the scale transformations

$$H = \frac{\lambda}{\mu^2} \tilde{F}, \quad \xi = \mu r \quad (\text{A.18})$$

we obtain

$$\left(\frac{d^2}{d\xi^2} + \frac{3}{\xi} \frac{d}{d\xi} \right)^2 H = H_0 + \frac{1}{6} H^3 \quad (\text{A.19})$$

where

$$H_0 \equiv \frac{\lambda}{\mu^2} \tilde{F}_0 = \frac{\lambda}{4\pi} \frac{\kappa_1(\xi)}{\xi}$$

$$\xrightarrow{\text{large } \xi} \frac{\lambda}{4\sqrt{2} \pi^{3/2}} \xi^{-3/2} e^{-\xi}. \quad (\text{A.20})$$

H obeys the boundary condition

$$\lim_{\xi \rightarrow \infty} H(\xi) = H_0(\xi). \quad (\text{A.21})$$

For large g , β also becomes large. We make a further transformation

$$\xi = \gamma + b \quad (\text{A.22})$$

where b is a large constant ($\sim \ln g$) to be defined soon. Ignoring terms $O(\frac{1}{b})$ or smaller, we can rewrite (A.19) as

$$\frac{d^4 H(\gamma)}{d\gamma^4} = \frac{\lambda}{4\sqrt{2} \pi^{3/2}} b^{-3/2} e^{-b} e^{-\gamma} + \frac{1}{6} H(\gamma)^3 \quad (\text{A. 23})$$

choosing b to obey

$$\lambda b^{-3/2} e^{-b} = 1, \quad (\text{A. 24})$$

we have

$$\frac{d^4 H}{d\gamma^4} = \frac{e^{-\gamma}}{4\sqrt{2} \pi^{3/2}} + \frac{1}{6} H^3 \quad (\text{A. 25})$$

and

$$\lim_{\gamma \rightarrow \infty} H(\gamma) = \frac{e^{-\gamma}}{4\sqrt{2} \pi^{3/2}}. \quad (\text{A. 26})$$

Since both the differential Eq. (A. 25) and the boundary condition (A. 26) are independent of λ , we conclude that the singularity γ_0 of H in Eq. (A. 25) and (A. 26) is a constant, independent of λ . Hence, the position of the singularity of \tilde{F} is at

$$\beta\mu = \gamma_0 + b \quad (\text{A. 27})$$

with

$$b + \frac{3}{2} \ln b = \ln \lambda. \quad (\text{A. 28})$$

To $O(\frac{1}{b})$, we can also express (A. 27) as

$$\beta\mu = \gamma_0' + b' \quad (\text{A. 29})$$

with

$$b' + \frac{3}{2} \ln b' = \ln g \quad (\text{A. 30})$$

and

$$\begin{aligned} \gamma_0' &= \gamma_0 + \ln [(12\pi)^2 \sqrt{48}] \\ &= \text{const.} \end{aligned} \quad (\text{A. 31})$$

Equations (A. 27) - (A. 31) describe the large g (or λ) behavior of β .

ACKNOWLEDGEMENTS

We wish to thank members of the particle theory group in Fermi National Accelerator Laboratory for their hospitality and for their inviting us as summer visitors where this investigation was completed.

FOOTNOTES AND REFERENCES

- ¹S. -J. Chang and Y. -P. Yao, "Non-Perturbative Approach to Infrared Behavior for $(\phi^3)_6$ and a Mechanism for Confinement," to appear in Phys. Rev. D. This work is referred to as Ref. 1 in the following.
- ²A. Zee, Phys. Rev. 7D, 3630 (1973).
- ³For example, A. Erdélye, et al., "Tables of Integral Transforms," McGraw-Hill Book Co. Inc. (1954).
- ⁴G. Mack, Lecture Notes in Physics, Vol. 17, 300 (1972); G. Woo and A. J. Mac Farlane, Nuc. Phys. B77, 91 (1974).
- ⁵D. Politzer, Phys. Rev. Lett. 30, 1346 (1973); D. J. Gross and F. Wilczek, Phys. Rev. Lett. 30 1343, (1973); G. 't Hooft, Remarks made at Marseille Conference (1973).
- ⁶S. -J. Chang and L. Tyburski, in preparation.

FIGURE CAPTIONS

- Fig. 1 The decay of a time-like gluon via a diagonal tree diagram.
- Fig. 2 Graphical representation for the integral equation obeyed by the diagonal tree diagrams.
- Fig. 3 The exponent $X_0 \equiv \beta\mu$ as a function of g .
- Fig. 4 The behavior of X_0 for small values of g .
Note the approximate linear dependence of $\ln X_0$ vs. $\frac{1}{g^2}$.
- Fig. 5 The average multiplicity $\langle n \rangle / (p/\mu) = g \, dX_0/dg$,
vs. g .
- Fig. 6 The multiplicity dispersion, $(\langle n^2 \rangle - \langle n \rangle^2) / (p/\mu)$
 $= (g \, d/dg)^2 X_0$, vs. g .

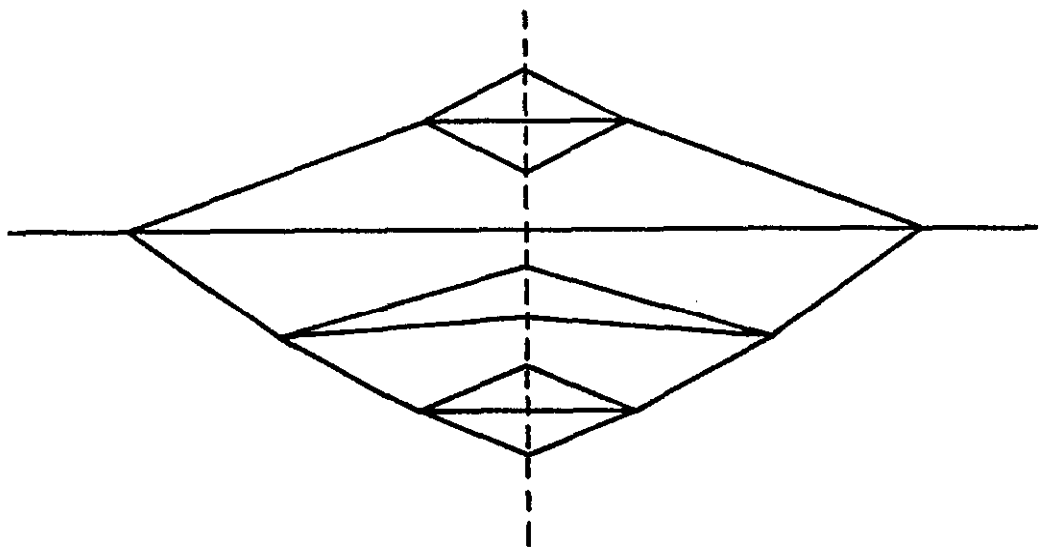


Fig. 1

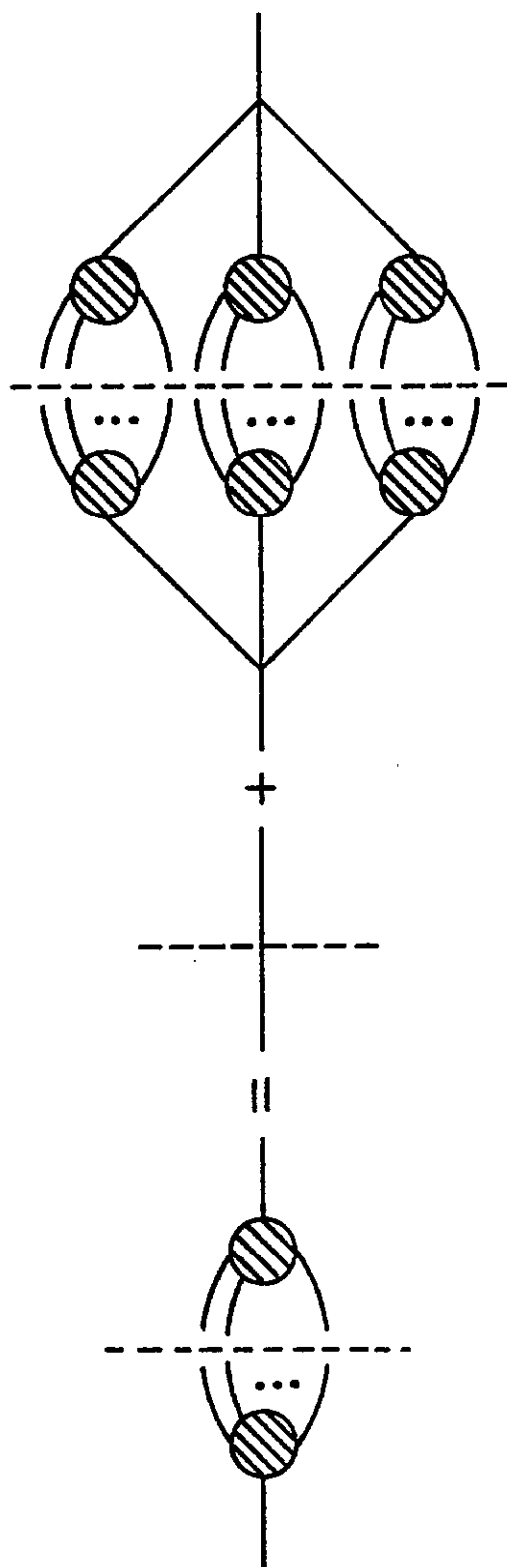


Fig. 2

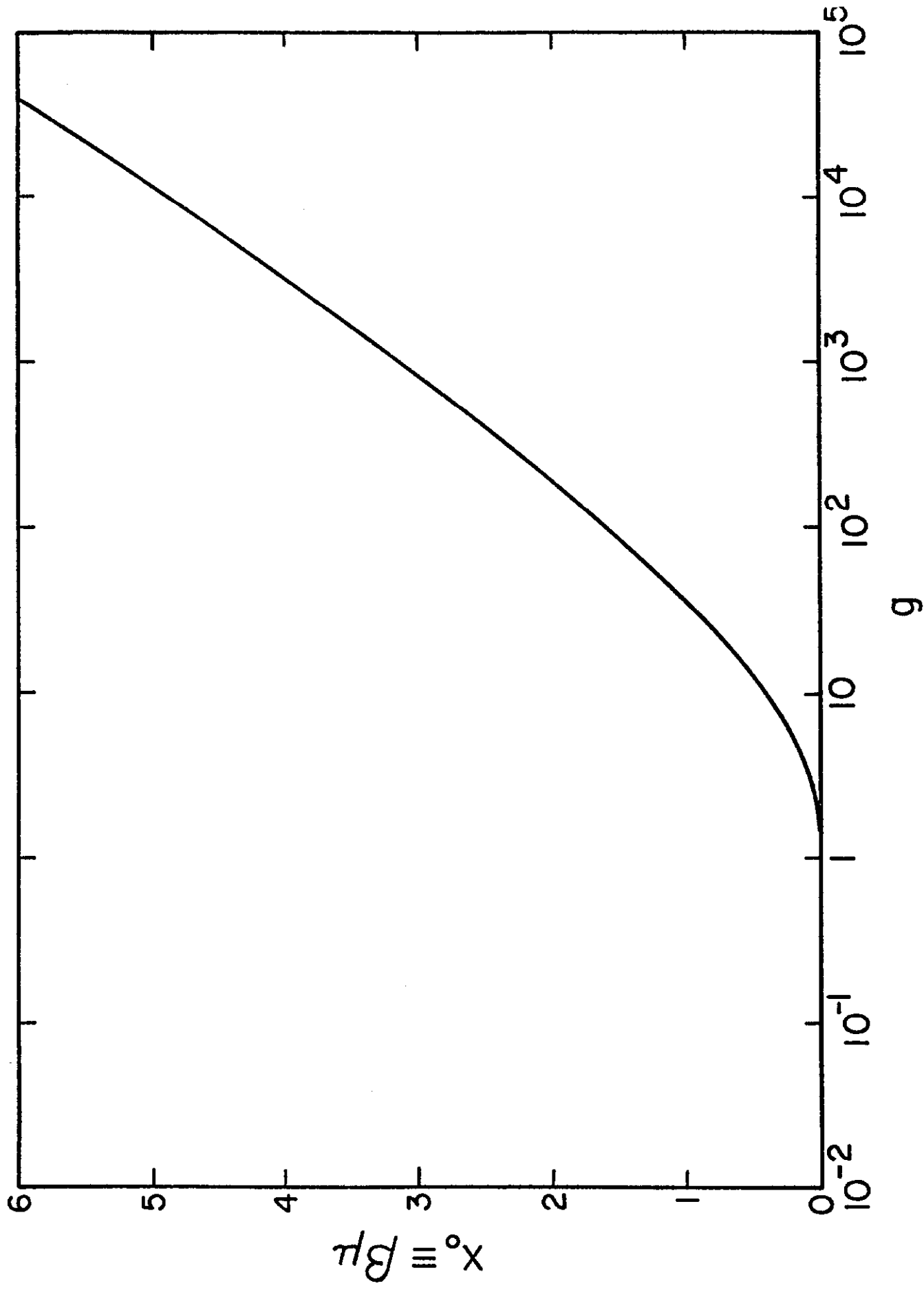
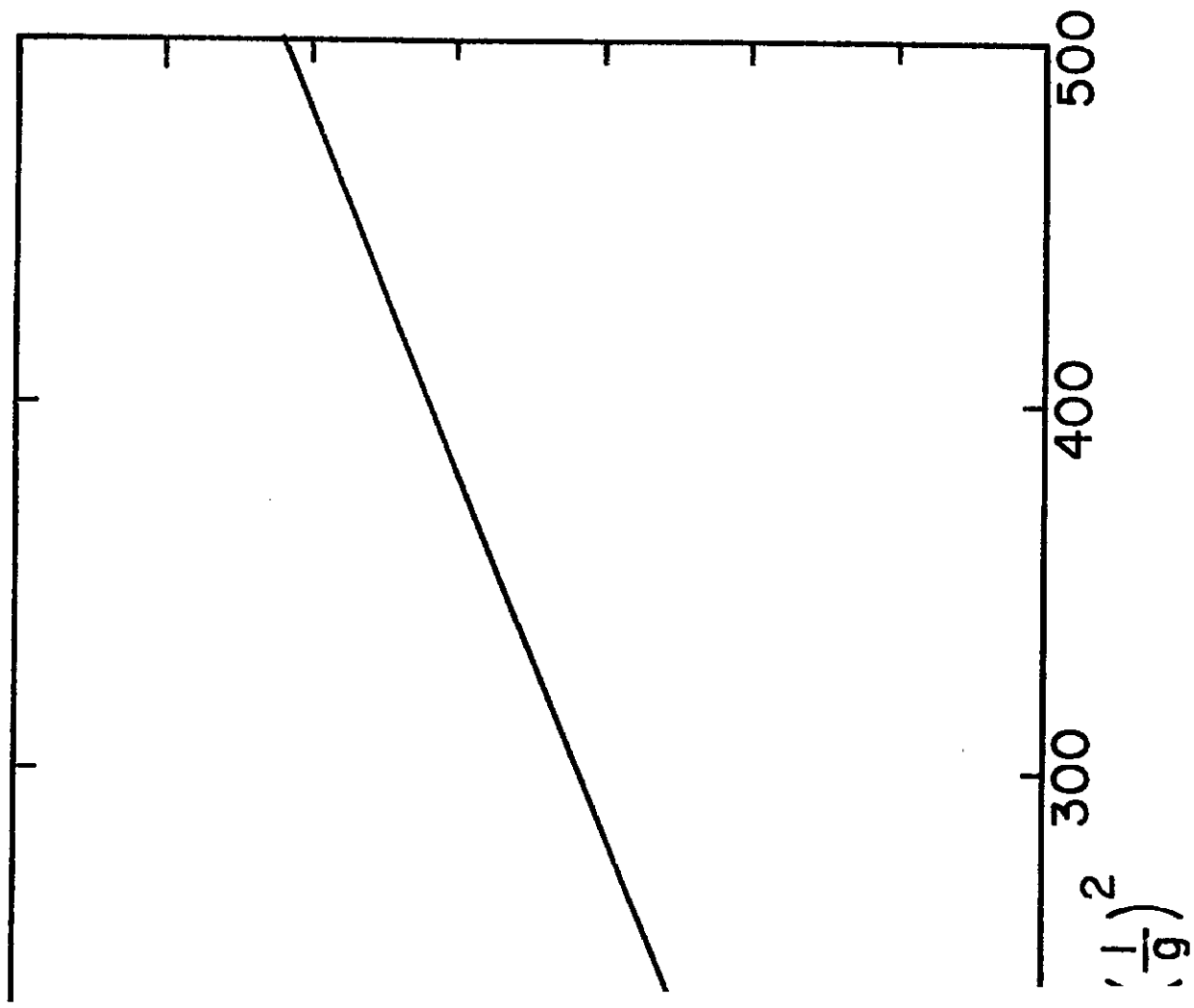


Fig. 3



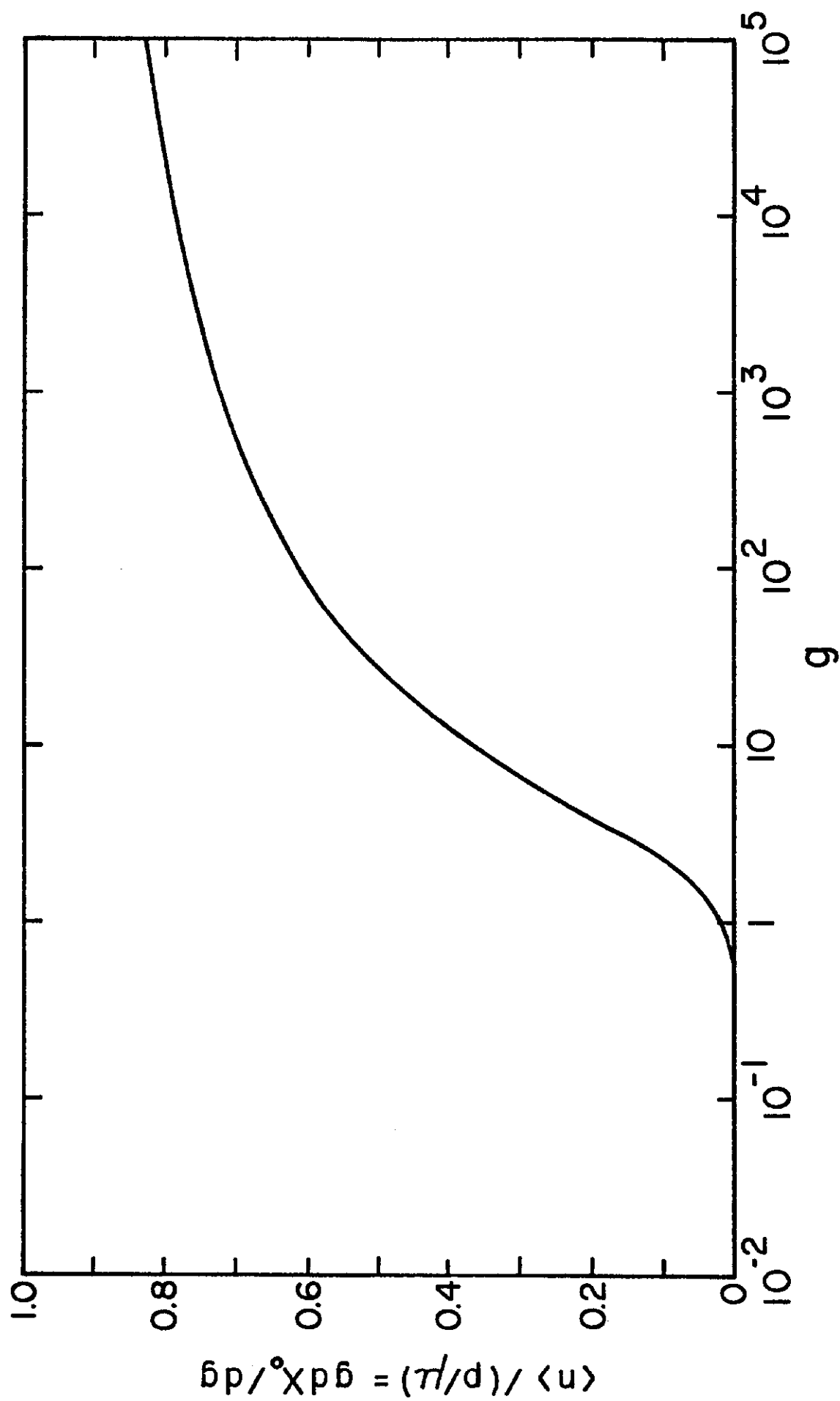


Fig. 5

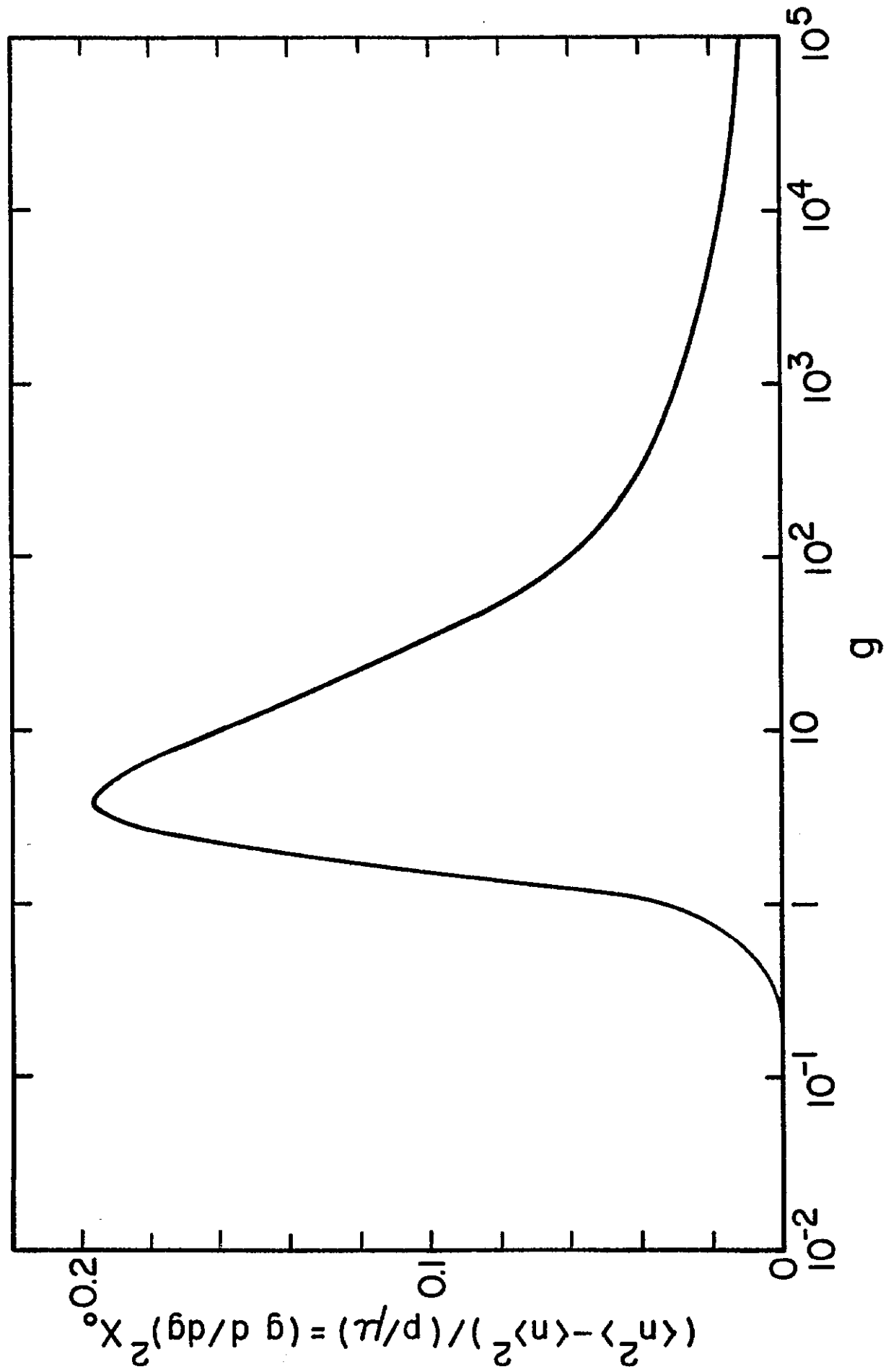


Fig. 6